

Masking Augmentation for Supervised Learning

Byeongho Heo Taekyung Kim Sangdoon Yun Dongyoon Han
NAVER AI Lab

Abstract

Pre-training using random masking has emerged as a novel trend in training techniques. However, supervised learning faces a challenge in adopting masking augmentations, primarily due to unstable training. In this paper, we propose a novel way to involve masking augmentations dubbed Masked Sub-model (MaskSub). MaskSub consists of the main-model and sub-model; while the former enjoys conventional training recipes, the latter leverages the benefit of strong masking augmentations in training. MaskSub addresses the challenge by mitigating adverse effects through a relaxed loss function similar to a self-distillation loss. Our analysis shows that MaskSub improves performance, with the training loss converging even faster than regular training, which suggests our method facilitates training. We further validate MaskSub across diverse training recipes and models, including DeiT-III, MAE fine-tuning, CLIP fine-tuning, ResNet, and Swin Transformer. Our results show that MaskSub consistently provides significant performance gains across all the cases. MaskSub provides a practical and effective solution for introducing additional regularization under various training recipes. Code available at <https://github.com/naver-ai/augsub>

1. Introduction

Supervised learning is the most basic and effective way to train a network to achieve high performance on a target task. To improve supervised learning, diverse regularizations are developed and used as training recipes [45, 47, 54], which represent a group of sophisticatedly tuned regularizations to maximize learning performance. Supervised learning has always held an advantage over self-supervised learning [4, 7] based on the benefit of supervision. However, emergence of Vision Transformer (ViT) [15] and Masked Image Modeling (MIM) [1, 21, 38] is changing this trends. ViT, which lacks inductive bias than convolution networks, poses a lot of challenges to generalization performance for supervised learning. On the other hand, MIMs such as MAE [21] rise as an alternative pre-training method for ViT by achieving competitive performance with supervised

learning recipes. Although a recent study [47] shows that new supervised learning outperforms MIMs, the gap is not significant. Thus, MIMs are still a strong competitor of supervised learning methods.

MIM masks random areas of an input image and forces the network to infer the masked area using the remaining area. A representative characteristic of MIM is high mask ratios over 50%. Although MIM also works at small mask ratios, it shows remarkable performance when trained with a high mask ratio. The high mask ratio is a major difference between MIM from supervised learning, since this high mask ratio, over 50%, is not allowed in supervised learning. Supervised learning also has utilized random masking as an augmentation [17, 66] but it significantly degrades performance when the masking ratio is high. In other words, supervised learning is not applicable for strong masking augmentation. We conjecture that it is a major problem of the current supervised learning recipe and there is room for improvement by enabling strong masking augmentation for supervised learning.

Our goal is to improve supervised learning with strong mask augmentation over 50% while maintaining the stability of training recipes. To this end, we introduce a training framework using a “sub-model” alongside the main-model; throughout this paper, we use the term “sub-model” to describe a partial model based on the “main-model”, in which some network features do not engage in training. The main-model uses standard training recipes [47, 54]. On the other hand, the sub-model utilizes mask augmentation. We name our method as Masked Sub-model (MaskSub). In the example of Figure 1, 50% random masking is applied to the sub-model as done in MAE [21]. As in Figure 1 (b), applying the 50% random masking to the main-model may lead to degraded performance. In contrast, as in Figure 1 (c), MaskSub utilizes the sub-model for random masking, and the sub-model receives a training signal from the main-model similar to the self-distillation [40, 62, 68]. While the random masking technique amplifies the difficulty of the training process, this is counterbalanced by self-distillation loss since the outputs of the main-model are relaxed and easier objective than the ground-truth label. In summary, MaskSub applies a mask augmentation separated from the

main-model, utilizing a relaxed loss form.

We analyze MaskSub using 100 epochs training on ImageNet [10]. Without MaskSub, loss convergence speed and corresponding accuracy are significantly degraded when mask augmentation is applied. Conversely, MaskSub successfully mitigates potential harmful effects from additional regularization, leading to a network training process that is even more efficient than standard training procedures. Also, MaskSub is not limited to mask augmentation and can be used for general drop regularizations. As a result, MaskSub is expanded to any random drop regularization without disrupting the convergence of original train loss; we employ three in-network drop-based options to show the applicability: masking [1, 21], dropout [44], and drop-path [16, 27]. Corresponding to each respective regularization strategy, we denote them MaskSub, DropSub, and PathSub. Among the three variants, MaskSub notably exhibits a significant enhancement in performance, which demonstrates necessity of mask augmentation in supervised learning.

We extensively validate the performance of MaskSub training. MaskSub is applied on various state-of-the-art supervised learning cases including DeiT-III [47], MAE fine-tuning [21], BEiTv2 finetuning [38], CLIP fine-tuning [14], ResNet-RSB [54], and Swin transformer [36]. MaskSub demonstrates remarkable performance improvement in all benchmarks. We argue that MaskSub can be regarded as a significant advancement as a novel way to utilize regularization for visual recognition.

2. Related Work

Training recipe has been considered an important ingredient in building a high-performance network. He et al. [22] demonstrate that the training recipe significantly influences the network performance. RSB [54] is a representative and high-performance recipe for ResNet. With the emergence of ViT [15], the training recipe for ViT has gained the attention of the field. DeiT [45] shows that ViT can be trained to strong performance with only ImageNet-1k [10]. DeiT-III [47] is an improved version of DeiT, which applies findings from RSB to DeiT instead of distillation from CNN teacher. It is challenging to implement stronger or additional regularization in existing training recipes. To address this issue, we propose MaskSub approach employing sub-models.

CoSub [48] introduces a similar concept to ours, utilizing sub-models. However, the objective of the sub-model differs significantly: while MaskSub aims to stabilize training through additional regularization, CoSub aims to train the sub-models in a collaborative manner [65]. We regard MaskSub as a more generalized framework since CoSub only considers the drop-path method to employ sub-models, whereas MaskSub can cover a variety of drop-based techniques including random masking.

Self-distillation utilizes supervision from a network itself

instead of using a teacher. ONE [68] uses a multi-branch ensemble to build superior output for the network and distill ensemble outputs as supervision for each branch. Some studies [40, 62] utilize the early-exit network for self-distillation. Those studies improve performance by using a full network as a teacher and an early-exit network as a student. MaskedKD [43] utilizes masking to reduce computation for knowledge distillation. From a self-distillation perspective, MaskSub presents a new insight to construct the student model (i.e., sub-model) from the teacher model (i.e., main-model) utilizing drop-based techniques. Note that most self-distillation studies are not compatible with recent training recipes [47, 54]. Thus, the general applicability of MaskSub is a significant contribution.

Self-supervised learning shares components with MaskSub. Previous works on contrastive learning incorporate two models with self-distillation loss [6, 18]. Want et al. [51] introduce a double tower with weak and strong augmentation for each model. In masked image models, supervised MAE [34] introduces additional supervised learning tasks to the MAE framework and accelerates MAE. Those studies partially share the fundamental concept with MaskSub and gave us the motivation. However, since training techniques applied to supervised learning are substantially different from techniques for self-supervised learning, MaskSub is significantly different from self-supervised learning approaches.

3. Method

We propose our method Masked Sub-model (MaskSub) with formulation and pseudo-code in Section 3.1. Section 3.2 presents analyses of MaskSub with loss convergence, accuracy, and gradient. In Section 3.3, we introduce variants of MaskSub: DropSub, and PathSub.

3.1. Masked Sub-model (MaskSub)

The cross-entropy loss with the softmax $\sigma(\mathbf{z}) = e^{z_i} / \sum_j e^{z_j}$ for images \mathbf{x}_i and one-hot labels $\mathbf{y}_i (i \in [1, 2, \dots, N])$ in a mini-batch with size N is denoted as

$$-\frac{1}{N} \sum_i \mathbf{y}_i \log(\sigma(f_\theta(\mathbf{x}_i | r_{\text{mask}} = 0))), \quad (1)$$

where f_θ represents the network used for training. r_{mask} means a ratio of masked patches in an input image. Since the masking ratio can be easily changed, we denote it as a condition for network function. Based on the value of r_{mask} , certain network features are dropped with probability r_{mask} . Note that we set the default masking ratio to zero for convenience. Then, loss for masking ratio $r \in [0, 1]$ is

$$-\frac{1}{N} \sum_i \mathbf{y}_i \log(\sigma(f_\theta(\mathbf{x}_i | r_{\text{mask}} = r))). \quad (2)$$

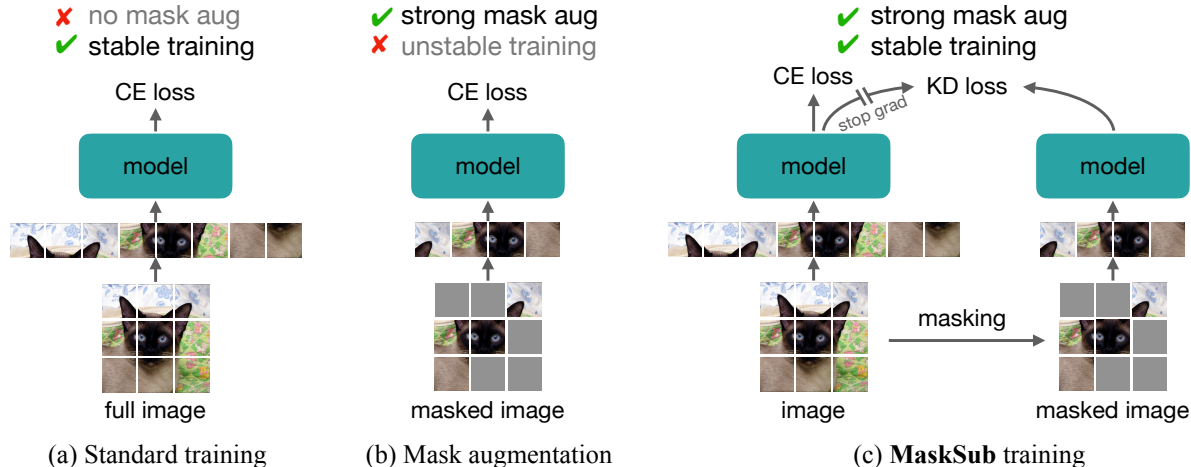


Figure 1. **Overview of Masked Sub-model (MaskSub)**. (a) standard supervised training; (b) masking augmentation training. The masking is applied to the main model, which degrades performance; (c) our **MaskSub** training, which separates the masking from the main model using the sub-model and relaxes loss with self-distillation. MaskSub substantially improves the state-of-the-art training recipes [47, 54].

Typically, a network with mask augmentation is trained with Eq. (2). But, we conjecture that training using Eq. (2) with high masking ratio (i.e. $r \geq 0.5$) may interfere with loss convergence and induce instability in training. To ensure training stability, we utilize the model output of equation Eq. (1), $f_\theta(\mathbf{x}_i|r_{\text{mask}} = 0)$, as guidance for masking augmentation $f_\theta(\mathbf{x}_i|r_{\text{mask}} = r)$ instead of \mathbf{y}_i . In other words, Eq. (2) is changed as

$$-\frac{1}{N} \sum_i \sigma(f_\theta(\mathbf{x}_i|r_{\text{mask}} = 0)) \log(\sigma(f_\theta(\mathbf{x}_i|r_{\text{mask}} = r))). \quad (3)$$

In our Masked Sub-model (MaskSub), the average of Eq. (1) and Eq. (3) is used as a loss function for the network. We designate $f_\theta(\mathbf{x}_i|r_{\text{mask}} = 0)$ as the main-model and $f_\theta(\mathbf{x}_i|r_{\text{mask}} = r)$ as the sub-model. This naming convention is employed because a network with masked inputs appears to be a subset of the entire network. In Eq. (3), the main-model output $f_\theta(\mathbf{x}_i|r_{\text{mask}} = 0)$ is used with stop-gradient. Thus, the sub-model is trained to mimic the main model, but we want the gradient for the main-model to be independent of the sub-model. This can be interpreted as self-distillation, where knowledge is transferred from the teacher (main-model) to the student (sub-model). Note that MaskSub can easily be expanded to binary cross-entropy loss by replacing the softmax function with the sigmoid function, which is used for recent training recipes [47, 54].

Algorithm 1 describes PyTorch-style pseudo-code of training with MaskSub. The masking ratio is put into the network input. The gradients are calculated on the average losses from the main and the sub-model. Note that MaskSub does not use any additional data augmentation, optimizer steps, and network parameters for the sub-model. In the implementation, we use MAE-style random masking [21], re-

Algorithm 1 MaskSub in PyTorch-style pseudo-code

```

for (x, label) in data_loader:
    o1 = f(x) # main model
    o2 = f(mask(x, r)) # sub-model (mask ratio: r)
    loss1 = CE(o1, label) / 2
    loss2 = CE(o2, softmax(o1.detach())) / 2
    (loss1+loss2).backward()
    optimizer.step()
  
```

moving masked tokens to reduce computation costs, by default. It significantly reduces the training cost of MaskSub. Approximately, MaskSub with 50% masking requires $\times 1.5$ computation to standard training. We will show the impact of MaskSub on diverse cases in Section 4, including computation analysis in Section A.1.

In MaskSub training, the sub-model mimics the main-model, and it automatically controls the difficulty of sub-model. If the main-model produces output closely aligned with the ground-truth label, the sub-model loss aims to attain an accurate classification output under masking augmentation. Conversely, if the main-model fails to converge, the sub-model loss becomes considerably easier than constructing a ground-truth label. In summary, MaskSub prioritizes the learning process, ensuring that masking augmentation is exclusively applied to images that produce successful output in a standard setting. We assert that the prioritized loss mechanism of MaskSub enables the network to preserve its convergence speed and learning stability while maintaining the benefits of masking augmentation.

3.2. Analysis

We analyze MaskSub with training ViT-B [15] for 100 epochs on ImageNet-1k [10]. Based on DeiT-III [47] training, we shorten the epoch to 100 epochs and use image resolution 224×224 . We compare three settings: standard,

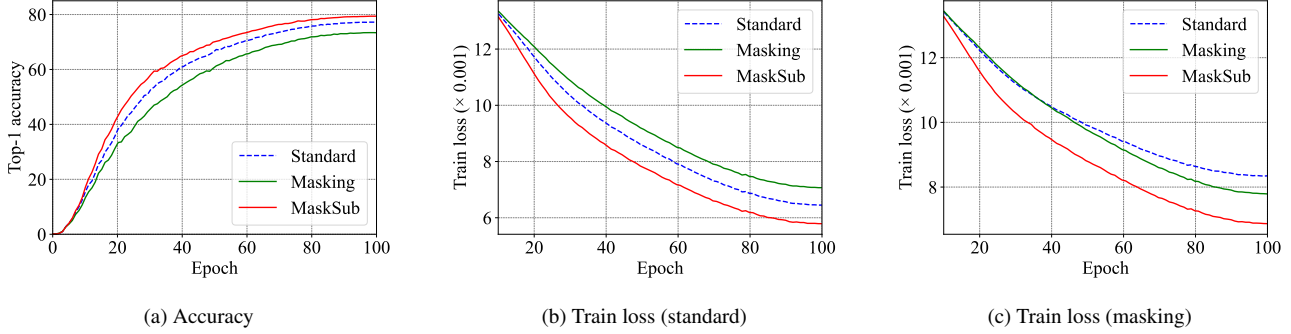


Figure 2. **MaskSub training analysis.** We use 50%-random masking to compare three training settings: standard Eq. (1), masking Eq. (2), and MaskSub. We visualize (a) accuracy on the validation set; (b) train loss without masking (standard); (c) train loss with masking.

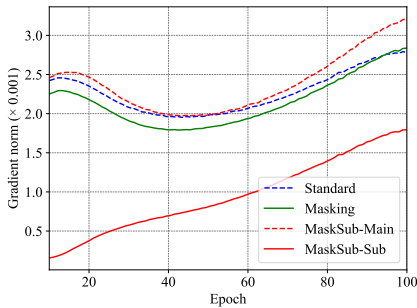


Figure 3. **Gradients magnitude of MaskSub.** The figure shows gradient norms for the main- and sub-model of MaskSub. The gradient norm is the averaged value over all parameters for an epoch.

masking, and MaskSub. The standard uses Eq. (1) as the training loss, and masking augmentation is not used. For the masking setting, the network is trained with Eq. (2). Note that it is a common practice to use a regularization or an augmentation in supervised learning. We compare those two settings with MaskSub. For analysis, we measured Eq. (1) ‘train loss - standard’ and Eq. (2) ‘train loss - masking’ regardless of loss used for training. It shows how losses changed by training setting.

Figure 2 shows loss and accuracy trends in random masking 50% (i.e. $r_{mask} = 0.5$) case. When random masking is applied to training (green), the masking loss (Figure 2c) converges better than the standard (blue). However, it significantly degrades the standard train loss (Figure 2b), resulting in a drop in accuracy (Figure 2a). Regularization over a certain strength often causes malicious effects on standard train loss, which decreases accuracy. As shown in Figure 2b and 2c, MaskSub improves the loss convergence for both losses: original and masking, which brings a significant improvement in accuracy.

Figure 3 explains the learning pattern between main-model and sub-model of MaskSub (Eq. (3)) in the aspect of gradients magnitude for training with random masking 50%. The gradient magnitude from the main-model (MaskSub-Main) is similar to that of other training. In con-

trast, gradients from the sub-model (MaskSub-Sub) have a small magnitude at the early stage. As the learning progresses, the gradients from the sub-model increase. It shows that MaskSub trains the network following our intention: automatic difficulty control. During the early stage of training, the gradients from the main-model lead the training. Following the progress of the main-model training, the sub-model adaptively increases its gradient magnitude and produces a reasonable amount of gradients at the end of training. In other words, the model training is relaxed from difficult masked inputs at the early stage, while it starts to learn masked input when the original inputs are sufficiently trained. We claim that the automatic difficulty control of MaskSub could be a general solution to introduce strong augmentation for supervised learning.

3.3. Expand to drop regularizations

We design MaskSub for masking augmentation. Due to its simplicity, it can be expanded to drop-based regularizations [17, 27, 44]. In this section, we introduce two variants of MaskSub: DropSub for dropout [44] and PathSub for drop-path [27]. Since the drop-based regularizations easily adjust their strength by controlling drop probability, MaskSub enables the model to learn strong drop regularization without degrading performance at standard loss, similar to masking augmentation. The performance of MaskSub variants is shown in Section 4.7 and A.4.

DropSub. Dropout [44] is a fundamental drop regularization. Dropout drops random elements of network features with a fixed probability. Since dropout is not related to feature structure, every element of the feature has independent drop probability p_{drop} . DropSub is simply implemented by changing r_{mask} to the dropout probability p_{drop} . Thus, the sub-model uses strong dropout, while the main-model follows a standard training recipe. Due to stability issues, dropout is not preferred in recent training recipes [45, 47]. However, DropSub enables strong dropout in ViT training and achieves performance improvement.

PathSub. Drop-path [16, 27] randomly drops a total feature

Network	400 epochs		800 epochs	
	DeiT-III	+ MaskSub	DeiT-III	+ MaskSub
ViT-S/16	80.4	81.1 (+0.7)	81.4	81.7 (+0.3)
ViT-B/16	83.5	84.1 (+0.6)	83.8	84.2 (+0.4)
ViT-L/16	84.5	85.2 (+0.7)	84.9	85.3 (+0.4)
ViT-H/14	85.1	85.7 (+0.6)	85.2	85.7 (+0.5)

Table 1. **Training from scratch with ViT using DeiT-III.** MaskSub (50%) is applied to the ViT training recipe [47] on ImageNet-1k. Note that the training settings are identical to the original ones.

of the network block with a probability p_{path} . PathSub is also implemented by changing r_{mask} to the drop-path probability p_{path} . Drop-path widely used in training recipes [45, 47, 54] to adjust the regularization strength [47]. Thus, different from previous cases, the main-model uses the drop-path following the training recipe, and the sub-model uses a higher drop probability than the main-model.

4. Experiments

We validate the effectiveness of Masked Sub-model (MaskSub) by applying it to diverse training scenarios. We claim MaskSub is an easy plug-in solution for various training recipes. Thus, we strictly follow the original training recipe, including optimizer parameters, learning rate and weight-decay, and regularization parameters. The only difference between baseline and MaskSub is the masking augmentation for the sub-model. We simply set the masking ratio of MaskSub to 50% across all experiments. In short, MaskSub does not have a hyper-parameter that varies depending on training scenarios.

4.1. Training from scratch

The training recipe in ViTs is a key factor enabling ViT to surpass CNN; thus, the ViT training recipe is a significant and active research topic. We use a state-of-the-art ViT recipe, DeiT-III [47], as a baseline. Integrating additional techniques into the DeiT-III is a significant challenge, and improvements made over DeiT-III can be considered a novel state-of-the-art in ViT training.

Various sizes of ViTs are trained with MaskSub (50%) on 400 and 800 epochs training. The results are shown in Table 1. MaskSub significantly improves performance in all settings. In 400 epochs training, MaskSub improves DeiT-III with substantial margins, which even outperforms 800 epochs DeiT-III except for ViT-S/16. MaskSub also demonstrates superior performance in 800 epochs. The impact of MaskSub is impressively sustained even for larger models like ViT-L/16 and ViT-H/16. It is worth noting that ViT-H + MaskSub (400 epochs) outperforms ViT-H/16 (800 epochs) with a significant +0.5pp gain even with half training length.

Network	Method	Epochs	Top-1 acc.
ViT-S	DeiT [45]	300	79.8
	MAE [21] [†]	1600	81.4
	DeiT-III [47]	800	81.4
	DeiT-III [47] + CoSub [48]	800	81.5
	DeiT-III [47] + MaskSub	800	81.7
ViT-B	DeiT [45]	300	81.8
	MAE [21]	1600	83.6
	DeiT-III [47]	800	83.8
	SupMAE [34]	400	83.6
	DeiT-III [47] + CoSub [48]	800	84.2
	DeiT-III [47] + MaskSub	400	84.1
	DeiT-III [47] + MaskSub	800	84.2
ViT-L	DeiT-III [47]	800	84.9
	DeiT-III [47] + CoSub [48]	800	85.3
	DeiT-III [47] + MaskSub	400	85.2
	DeiT-III [47] + MaskSub	800	85.3
ViT-H	DeiT-III [47]	800	85.2
	DeiT-III [47] + CoSub [48]	800	85.7
	DeiT-III [47] + MaskSub	400	85.7

Table 2. **Comparison with pre-training methods.** We compared DeiT-III [47] + MaskSub with various pre-training methods. MaskSub shows remarkable performance in all sizes.

	Epochs	Network	Baseline	+MaskSub
MAE [21] finetuning	100	ViT-B/16	83.6	83.9 (+0.3)
	50	ViT-L/16	85.9	86.1 (+0.2)
	50	ViT-H/14	86.9	87.2 (+0.3)
BEiTv2 [38] finetuning	100	ViT-B/16	85.5	85.6 (+0.1)
	50	ViT-L/16	87.3	87.4 (+0.1)
CLIP [41] finetuning	50	ViT-B/16	84.8	85.2 (+0.4)
	30	ViT-L/14	87.5	87.8 (+0.3)

Table 3. **ImageNet-1k finetuning.** We report finetuned performance of MAE [21], BEiT v2 [38] and CLIP finetuning [14] with MaskSub (50%). Official pretrained weights are used.

Thus, MaskSub is an effective way to improve ViT training.

Table 2 shows performances of MaskSub compared to other pre-training methods. With a reasonable performance gap, MaskSub outperforms MAE [21] in ViT-S and ViT-B. Compared to SupMAE [34], MaskSub achieves better performance with the same training epoch. CoSub [48] has comparable performance with MaskSub but, as shown in Section 4.4, MaskSub requires less computation costs than CoSub. Thus, we argue that MaskSub outperforms CoSub.

4.2. Finetuning

Following the emergence of self-supervised learning [21] and visual-language model [41], the significance of finetuning has notably increased. Generally, self-supervised learning, such as MAE [21] and BEiT [1, 38], does not use su-

Network	Method	Top-1 acc.
CLIP-B	Linear probing [41]	80.2
	Finetuning [14]	84.8
	Finetuning [14] + MaskSub	85.2
ViT-B	FD-CLIP [53]	84.9
	MaskDistill [39]	85.5
	MVP [52]	84.4
	MILAN [26]	85.4
	CAEv2 [64]	85.5
	BEiTv2 [38]	85.5
	BEiTv2 [38] + MaskSub	85.6

Table 4. **Comparison with CLIP-based training on ImageNet-1k.** Our finetuning experiment is close to the state-of-the-art of ViT-B training. MaskSub applied to BEiTv2 [38] fine-tuning outperforms cutting-edge studies on CLIP-based training.

pervised labels at pretraining, which makes MaskSub inapplicable for pretraining. However, most methods utilize supervised finetuning steps after pretraining to demonstrate their performance. Thus, we apply our MaskSub (50%) to the finetuning stage to verify the effect of MaskSub on finetuning. Note that we strictly follow original recipes and apply MaskSub (50%) based on it. All finetuning is conducted using officially released pretrained weights.

We utilize three finetuning recipes: MAE [21], BEiT v2 [38], and Finetune CLIP [14]. MAE [21] is a representative method of masked image models (MIM). Since our random masking is motivated by MAE, MaskSub is seamlessly integrated into MAE finetuning process. BEiT v2 [38] utilizes pretrained CLIP for MIM and achieves superior performance compared to MAE. Following the masking strategy of BEiT v2 using mask-token, we adjust MaskSub to masking using mask-token from the pretrained weight instead of MAE-style masking. Finetune CLIP [14] is a finetuning recipe for CLIP [41] pretrained weights. MaskSub is applied to finetuning CLIP without change.

Table 3 shows the finetuning results. MaskSub improves the performance of all finetune recipes, including large-scale ViT models. This is notable as it shows substantial improvement with a short finetuning phase of fewer than 100 epochs compared to the pretraining period of 1600 epochs. In MAE finetuning, MaskSub improves 0.2 - 0.3pp in all model sizes. MaskSub is also effective on BEiT v2, which utilizes RPE [1, 36] and masking strategy with mask-token. Even in CLIP finetuning, MaskSub achieves substantial improvement. In finetuning CLIP, we report performance at the last epoch rather than selecting the best performance in early epochs. The best performance of finetuning CLIP with MaskSub is the same as the baseline. Table 4 demonstrates the impacts of MaskSub compared to cutting-edge CLIP-based training recipes. It shows that MaskSub improves the performance of state-of-the-art training recipes.

Recipe	Epochs	Network	Baseline	+ MaskSub
RSB A2 [54]	300	ResNet50	79.7	80.0 (+0.3)
		ResNet101	81.4	82.1 (+0.7)
		ResNet152	81.8	82.8 (+1.0)
Swin [36]	300	Swin-T	81.3	81.4 (+0.1)
		Swin-S	83.0	83.4 (+0.4)
		Swin-B	83.5	83.9 (+0.4)

Table 5. **ImageNet-1k with hierarchical architecture.** We show the performance of ResNet [19] and Swin Transformer [36] trained from scratch with MaskSub (50%).

Network	Method	Top-1 acc.
ResNet50	Baseline [20]	76.1
	ResNeXt50 [58] + ONE [68]	78.2
	BYOT [62]	75.2
	Self-Distillation [63]	78.3
	MixSKD [59]	78.8
	RSB [54] + MaskSub	80.0
ResNet101	Baseline [20]	77.4
	Self-Distillation [63]	78.9
	RSB [54] + MaskSub	82.1
ResNet152	Baseline [20]	78.3
	PS-KD [28]	79.2
	Self-Distillation [63]	80.6
	SD-dropout [32]	75.5
	RSB [54] + MaskSub	82.8

Table 6. **Comparison with self-distillation methods.** Based on ResNet performance, we compare MaskSub with various self-distillation methods.

4.3. Hierarchical architecture

We extend experiments to architectures with hierarchical spatial dimensions: ResNet [19] and Swin Transformer [36]. Unlike ViT maintains spatial token length for all layers, those networks change the spatial size of features in the middle of layers, requiring a change in masking strategy. We apply MaskSub (50%) to ResNet and Swin Transformer. We simply fill out masked regions with zero pixels for ResNets and replace masked regions with mask-tokens for Swin Transformer. It maintains the spatial structure and enables spatial size reduction of hierarchical architecture. Following a literature [55], we use random masking with patch-size 32×32 . Note that the computation reduction using MAE-style masking is not applicable for this case. Thus, MaskSub costs double the training budget. For ResNet, we use a high-performance training recipe [54] with 300 epochs. The recipe of original paper [36] is used for the Swin Transformer training. We strictly follow the training recipe and apply MaskSub without recipe tuning.

Results are shown in Table 5. MaskSub achieves impressive performance gains even in ResNet and Swin Trans-

Architecture	+MaskSub	Epochs	GPU days	Accuracy
ViT-S/16	-	600	22	80.7
	✓	400	22	81.2 (+0.5)
ViT-B/16	-	600	26	83.7
	✓	400	25	84.1 (+0.4)
ResNet101	-	600	24	81.5
	✓	300	20	82.1 (+0.6)
ResNet152	-	600	32	82.0
	✓	300	29	82.8 (+0.8)

Table 7. **Comparison in the same training budget.** All training has been conducted with NVIDIA V100 8 GPUs. GPU days refer to the number of days required for training when using a single V100 GPU.

former. ResNet and Swin are substantially different architectures from ViT. Thus, the result implies that the effectiveness of MaskSub is not limited to ViT architectures and is applicable to hierarchical architectures. Using ResNet results, we compare MaskSub with various self-distillation methods. As shown in Table 6, most of the self-distillations report performance based on weak training recipes. Thus, they are incompatible with cutting-edge training recipes such as RSB [54], which limits the general applicability of self-distillation. Otherwise, MaskSub can easily be plugged into strong training recipes and contribute to achieving state-of-the-art performance.

4.4. Training budget

We have shown that MaskSub effectively improves the performance of various architectures. However, MaskSub requires additional computation costs for the sub-model, which increases training costs. Thus, we analyze MaskSub regarding its training costs to determine if MaskSub could be an effective solution within a limited training budget. We compare MaskSub with training recipes with increased epochs to align with the training budget. The training budget is quantified regarding required GPU days when only a single NVIDIA V100 GPU is used for training. Table 7 shows the results. In ViT training, MaskSub outperforms baseline with $\times 1.5$ epochs setting. Thus, MaskSub is superior to the long epoch training to spend computation costs for training ViT. For ResNet, we compare 300 epochs MaskSub with 600 epochs training recipe RSB [54] A1. MaskSub outperforms 600 epochs training recipes in ResNet101 and ResNet152. Consequently, the results show that MaskSub is an effective way to improve training, even considering computation costs for the sub-model.

We compare MaskSub with other methods for an additional augmentation: DataAugment [25], GradAug [60], and CoSub [48]. DataAugment [25] uses doubled data augmentations for the same image which is similar to con-

Method	Accuracy	GPU days
Baseline [47]	83.5	17.3
DataAugment [25]	83.5 (+0.0)	36.8 (+113%)
GradAug [60]	83.2 (-0.3)	39.7 (+129%)
CoSub [48]	83.9 (+0.4)	35.3 (+104%)
MaskSub	84.1 (+0.6)	25.1 (+45%)

Table 8. **Comparison in ImageNet-1k training.** The table shows performance and GPU costs of augmenting methods for ViT-B 400 epoch training.

Method	Accuracy	GPU days
Baseline [47]	83.6	6.0
DataAugment [25]	83.1 (-0.5)	11.8 (+97%)
GradAug [60]	84.0 (+0.4)	23.4 (+290%)
CoSub [48]	83.8 (+0.2)	11.0 (+83%)
MaskSub	83.9 (+0.3)	8.6 (+43%)

Table 9. **Comparison in MAE finetuning.** The table displays performances and GPU costs of augmenting methods when applied to MAE ViT-B fine-tuning.

trastive learning [4, 7]. GradAug [2020] utilizes a network pruning [61] to build sub-network. CoSub introduces a sub-network based on drop-path [27] and uses the sub-network as mutual learning [65]. Table 8 shows the 400 epoch training from scratch result, and Table 9 represents MAE fine-tuning result. Note that GradAug in Table 8 is 200 epochs training result to adjust computation cost similar to other methods. All augmentation methods require additional computation costs. In particular, GradAug spends almost 300% of additional training costs compared to original training. On the other hand, our MaskSub only requires a small amount of additional costs (below 50%), which is a remarkable advantage in training. With the smallest computation, our MaskSub achieves substantial performance improvements. MaskSub performs superior to CoSub in all cases and performs similarly to GradAug in MAE fine-tuning with 1/6 training costs.

4.5. Transfer learning

Improvement in pretraining can boost the performance of downstream tasks [29]. We measure the transfer learning performance of MaskSub using 800 epochs pretrained weight from Table 1. CIFAR-10 [31], CIFAR-100 [31], Oxford Flowers-102 [37], Stanford Cars [30] and iNaturalist [49] are used for finetuning datasets. We use the AdamW training recipe [47] and also evaluate performance when MaskSub (50%) is applied to the finetuning process. Table 10 shows the results. The backbone pretrained with MaskSub consistently outperforms the DeiT-III backbone across all cases. Moreover, when MaskSub is applied to the

Model	Pretraining + MaskSub	Finetuning + MaskSub	CIFAR-10 [31]	CIFAR-100 [31]	Flowers [37]	Cars [30]	iNat-18 [49]	iNat-19 [49]
ViT-S/16	-	-	98.8	90.0	94.5	80.9	70.1	76.7
	✓	-	98.9 (+0.1)	90.6 (+0.6)	95.2 (+0.7)	81.2 (+0.3)	70.8 (+0.7)	77.0 (+0.3)
	✓	✓	98.8 (+0.0)	89.9 (-0.1)	98.3 (+3.8)	92.2 (+1.3)	71.2 (+1.1)	77.1 (+0.4)
ViT-B/16	-	-	99.1	91.7	97.5	90.0	73.2	78.5
	✓	-	99.2 (+0.1)	91.9 (+0.2)	97.7 (+0.2)	90.2 (+0.2)	73.6 (+0.4)	78.8 (+0.3)
	✓	✓	98.8 (-0.3)	89.6 (-2.1)	98.7 (+1.2)	92.8 (+2.8)	73.9 (+0.7)	79.1 (+0.6)

Table 10. **Transfer learning to small-scale datasets.** Table shows transfer learning performance with/without MaskSub. We measure the performance when MaskSub is applied to pretraining and finetuning. The standard deviations over three runs are reported in Table A.9.

Model	+MaskSub	MNLI	QQP	QNLI	SST-2	CoLA	STS-B	MRPC	RTE	Avg.	Training method	ImageNet-1k Zero-shot acc.
BERT [12]	-	84.1	87.5	91.0	91.6	54.7	87.0	88.5	62.8	80.9	CLIP [41]	33.5
<i>base</i>	✓	84.5	87.7	91.3	91.9	58.3	86.8	89.2	63.2	81.6		CLIP [41] + Masking
BERT [12]	-	86.8	88.2	92.3	93.8	63.3	89.3	92.0	69.7	84.4	CLIP [41] + MaskSub	37.6 (+4.1)
<i>large</i>	✓	87.1	89.0	92.7	94.0	65.2	88.6	91.5	69.3	84.7		

Table 11. **GLUE [50] benchmark with BERT [12].** We apply MaskSub on GLUE benchmark to validate the effect of MaskSub on language model finetuning.

Table 12. **MaskSub on CLIP pretraining** with CLIP ViT-B/32 models.

finetuning process, it further boosts performance in most cases except CIFAR [31].

4.6. Beyond image classification

Masking augmentation like MIM originates from a language training method [12]. It implies that MaskSub might be applicable to language domains similar to computer vision tasks. To verify general applicability, we apply MaskSub to two additional tasks beyond image classification: GLUE [50] benchmark and CLIP [41] pretraining. The first task is a text-classification benchmark GLUE [50]. We use BERT [12] as a pretrained model and apply MaskSub with 15% masking following the masking ratio of BERT. As shown in Table 11, MaskSub improves text-classification performance. MaskSub is also applied to CLIP [41] pretraining. Table 12 shows the results. CLIP trained with MaskSub (50%) shows improved zero-shot performance. Experimental details are in Section B. These results verify that MaskSub has significant impacts not only vision domain but also language and vision&language domain.

4.7. Extending to drop regularizations

In Section 3.3, we propose MaskSub variants expanded to drop-related regularizations [27, 44]. We validate the performance of MaskSub variants on a 400 epochs training with Deit-III. We use masking [21] (50%), dropout [44] (0.2), and drop-path [27] (baseline + 0.1) for MaskSub, DropSub, and PathSub, respectively. Table 13 shows the results. Variants of MaskSub outperform the baseline. Among the three, MaskSub shows the best performance. Also, MaskSub has the lowest computation costs due to

Architecture	Baseline	MaskSub	DropSub	PathSub
ViT-S/16	80.4	81.1 (+0.7)	80.6 (+0.2)	80.8 (+0.4)
ViT-B/16	83.5	84.1 (+0.6)	83.8 (+0.3)	83.8 (+0.3)
Computational costs	×1.0	×1.5	×2.0	×2.0

Table 13. **Comparison of MaskSub variants.** We validate drop-based variants of MaskSub: DropSub, and PathSub.

MAE [21]-style computation reduction. Thus, we conclude that MaskSub (50%) is the best in practice compared to variants with drop regularizations. Additional results are reported in Table A.5.

5. Conclusion

In this work, we have presented a new way to introduce masking augmentation to supervised learning. Our method, Masked Sub-model (MaskSub), is designed to leverage masking augmentation within a sub-model, which is separated from main training and uses a relaxed loss function. Our extensive analysis reveals that MaskSub effectively mitigates malicious effects of heavy masking while accelerating the convergence speed, yielding superior performance. We verify MaskSub on various training recipes, including diverse architecture. Notably, MaskSub demonstrates significant performance improvements across diverse scenarios. We claim that MaskSub is a substantial advancement in training recipes and contributes to building novel augmentation strategies.

References

- [1] Hangbo Bao, Li Dong, Songhao Piao, and Furu Wei. Beit: Bert pre-training of image transformers. *arXiv preprint arXiv:2106.08254*, 2021. **1, 2, 5, 6**
- [2] Andrei Barbu, David Mayo, Julian Alverio, William Luo, Christopher Wang, Dan Gutfreund, Josh Tenenbaum, and Boris Katz. Objectnet: A large-scale bias-controlled dataset for pushing the limits of object recognition models. *Advances in neural information processing systems*, 32, 2019. **13**
- [3] Zhaowei Cai and Nuno Vasconcelos. Cascade r-cnn: high quality object detection and instance segmentation. *IEEE Transactions on Pattern Analysis and Machine Intelligence*, 43(5):1483–1498, 2019. **13**
- [4] Mathilde Caron, Hugo Touvron, Ishan Misra, Hervé Jégou, Julien Mairal, Piotr Bojanowski, and Armand Joulin. Emerging properties in self-supervised vision transformers. In *Proceedings of the IEEE/CVF international conference on computer vision*, pages 9650–9660, 2021. **1, 7**
- [5] Soravit Changpinyo, Piyush Sharma, Nan Ding, and Radu Soricut. Conceptual 12M: Pushing web-scale image-text pre-training to recognize long-tail visual concepts. In *CVPR*, 2021. **16**
- [6] Xinlei Chen and Kaiming He. Exploring simple siamese representation learning. In *Proceedings of the IEEE/CVF Conference on Computer Vision and Pattern Recognition*, pages 15750–15758, 2021. **2**
- [7] Xinlei Chen, Saining Xie, and Kaiming He. An empirical study of training self-supervised vision transformers. In *Proceedings of the IEEE/CVF international conference on computer vision*, pages 9620–9629, 2021. **1, 7**
- [8] MMCV Contributors. MMCV: OpenMMLab computer vision foundation. <https://github.com/open-mmlab/mmcv>, 2018. **16**
- [9] MMSegmentation Contributors. MMSegmentation: Openmmlab semantic segmentation toolbox and benchmark. <https://github.com/open-mmlab/mms Segmentation>, 2020. **16**
- [10] Jia Deng, Wei Dong, Richard Socher, Li-Jia Li, Kai Li, and Li Fei-Fei. Imagenet: A large-scale hierarchical image database. In *Proceedings of the IEEE/CVF Conference on Computer Vision and Pattern Recognition*, pages 248–255. Ieee, 2009. **2, 3**
- [11] Karan Desai, Gaurav Kaul, Zubin Aysola, and Justin Johnson. RedCaps: Web-curated image-text data created by the people, for the people. In *NeurIPS Datasets and Benchmarks*, 2021. **16**
- [12] Jacob Devlin, Ming-Wei Chang, Kenton Lee, and Kristina Toutanova. Bert: Pre-training of deep bidirectional transformers for language understanding. *arXiv preprint arXiv:1810.04805*, 2018. **8, 16**
- [13] Josip Djolonga, Jessica Yung, Michael Tschannen, Rob Romijnders, Lucas Beyer, Alexander Kolesnikov, Joan Puigcerver, Matthias Minderer, Alexander D’Amour, Dan Moldovan, et al. On robustness and transferability of convolutional neural networks. In *Proceedings of the IEEE/CVF Conference on Computer Vision and Pattern Recognition*, pages 16458–16468, 2021. **13**
- [14] Xiaoyi Dong, Jianmin Bao, Ting Zhang, Dongdong Chen, Shuyang Gu, Weiming Zhang, Lu Yuan, Dong Chen, Fang Wen, and Nenghai Yu. Clip itself is a strong fine-tuner: Achieving 85.7% and 88.0% top-1 accuracy with vit-b and vit-l on imagenet. *arXiv preprint arXiv:2212.06138*, 2022. **2, 5, 6**
- [15] Alexey Dosovitskiy, Lucas Beyer, Alexander Kolesnikov, Dirk Weissenborn, Xiaohua Zhai, Thomas Unterthiner, Mostafa Dehghani, Matthias Minderer, Georg Heigold, Sylvain Gelly, et al. An image is worth 16x16 words: Transformers for image recognition at scale. *arXiv preprint arXiv:2010.11929*, 2020. **1, 2, 3**
- [16] Angela Fan, Edouard Grave, and Armand Joulin. Reducing transformer depth on demand with structured dropout. *arXiv preprint arXiv:1909.11556*, 2019. **2, 4**
- [17] Golnaz Ghiasi, Tsung-Yi Lin, and Quoc V Le. Dropblock: A regularization method for convolutional networks. *Advances in neural information processing systems*, 31, 2018. **1, 4**
- [18] Jean-Bastien Grill, Florian Strub, Florent Altché, Corentin Tallec, Pierre Richemond, Elena Buchatskaya, Carl Doersch, Bernardo Avila Pires, Zhaohan Guo, Mohammad Gheshlaghi Azar, et al. Bootstrap your own latent—a new approach to self-supervised learning. *Advances in neural information processing systems*, 33:21271–21284, 2020. **2**
- [19] Kaiming He, Xiangyu Zhang, Shaoqing Ren, and Jian Sun. Deep residual learning for image recognition. In *Proceedings of the IEEE conference on computer vision and pattern recognition*, pages 770–778, 2016. **6**
- [20] Kaiming He, Xiangyu Zhang, Shaoqing Ren, and Jian Sun. Deep residual learning for image recognition. In *Proceedings of the IEEE conference on computer vision and pattern recognition*, pages 770–778, 2016. **6**
- [21] Kaiming He, Xinlei Chen, Saining Xie, Yanghao Li, Piotr Dollár, and Ross Girshick. Masked autoencoders are scalable vision learners. In *Proceedings of the IEEE/CVF Conference on Computer Vision and Pattern Recognition*, pages 16000–16009, 2022. **1, 2, 3, 5, 6, 8, 14, 15**
- [22] Tong He, Zhi Zhang, Hang Zhang, Zhongyue Zhang, Junyuan Xie, and Mu Li. Bag of tricks for image classification with convolutional neural networks. In *Proceedings of the IEEE/CVF Conference on Computer Vision and Pattern Recognition*, pages 558–567, 2019. **2**
- [23] Dan Hendrycks, Steven Basart, Norman Mu, Saurav Kadavath, Frank Wang, Evan Dorundo, Rahul Desai, Tyler Zhu, Samyak Parajuli, Mike Guo, et al. The many faces of robustness: A critical analysis of out-of-distribution generalization. In *Proceedings of the IEEE/CVF International Conference on Computer Vision*, pages 8340–8349, 2021. **13**
- [24] Dan Hendrycks, Kevin Zhao, Steven Basart, Jacob Steinhardt, and Dawn Song. Natural adversarial examples. In *Proceedings of the IEEE/CVF Conference on Computer Vision and Pattern Recognition*, pages 15262–15271, 2021. **13**
- [25] Elad Hoffer, Tal Ben-Nun, Itay Hubara, Niv Giladi, Torsten Hoefler, and Daniel Soudry. Augment your batch: Improving generalization through instance repetition. In *Proceedings of*

- the IEEE/CVF Conference on Computer Vision and Pattern Recognition*, pages 8129–8138, 2020. 7
- [26] Zejiang Hou, Fei Sun, Yen-Kuang Chen, Yuan Xie, and Sun-Yuan Kung. Milan: Masked image pretraining on language assisted representation. *arXiv preprint arXiv:2208.06049*, 2022. 6
- [27] Gao Huang, Yu Sun, Zhuang Liu, Daniel Sedra, and Kilian Q Weinberger. Deep networks with stochastic depth. In *Proceedings of the European Conference on Computer Vision*, pages 646–661. Springer, 2016. 2, 4, 7, 8, 14, 15, 16
- [28] Kyungyul Kim, ByeongMoon Ji, Doyoung Yoon, and Sangheum Hwang. Self-knowledge distillation with progressive refinement of targets. In *Proceedings of the IEEE/CVF international conference on computer vision*, pages 6567–6576, 2021. 6
- [29] Simon Kornblith, Jonathon Shlens, and Quoc V Le. Do better imagenet models transfer better? In *Proceedings of the IEEE/CVF Conference on Computer Vision and Pattern Recognition*, pages 2661–2671, 2019. 7
- [30] Jonathan Krause, Michael Stark, Jia Deng, and Li Fei-Fei. 3d object representations for fine-grained categorization. In *Proceedings of the IEEE international conference on computer vision workshops*, pages 554–561, 2013. 7, 8
- [31] Alex Krizhevsky, Geoffrey Hinton, et al. Learning multiple layers of features from tiny images. 2009. 7, 8
- [32] Hyoje Lee, Yeachan Park, Hyun Seo, and Myungjoo Kang. Self-knowledge distillation via dropout. *Computer Vision and Image Understanding*, 233:103720, 2023. 6
- [33] Yanghao Li, Hanzi Mao, Ross Girshick, and Kaiming He. Exploring plain vision transformer backbones for object detection. In *Proceedings of the European Conference on Computer Vision*, pages 280–296. Springer, 2022. 13, 16
- [34] Feng Liang, Yangguang Li, and Diana Marculescu. Supmae: Supervised masked autoencoders are efficient vision learners. *arXiv preprint arXiv:2205.14540*, 2022. 2, 5
- [35] Tsung-Yi Lin, Michael Maire, Serge Belongie, James Hays, Pietro Perona, Deva Ramanan, Piotr Dollár, and C Lawrence Zitnick. Microsoft coco: Common objects in context. In *Proceedings of the European Conference on Computer Vision*, pages 740–755. Springer, 2014. 13, 16
- [36] Ze Liu, Yutong Lin, Yue Cao, Han Hu, Yixuan Wei, Zheng Zhang, Stephen Lin, and Baining Guo. Swin transformer: Hierarchical vision transformer using shifted windows. In *Proceedings of the IEEE/CVF International Conference on Computer Vision*, pages 10012–10022, 2021. 2, 6
- [37] Maria-Elena Nilsback and Andrew Zisserman. Automated flower classification over a large number of classes. In *2008 Sixth Indian Conference on Computer Vision, Graphics & Image Processing*, pages 722–729. IEEE, 2008. 7, 8
- [38] Zhiliang Peng, Li Dong, Hangbo Bao, Qixiang Ye, and Furu Wei. Beit v2: Masked image modeling with vector-quantized visual tokenizers. *arXiv preprint arXiv:2208.06366*, 2022. 1, 2, 5, 6, 13, 16
- [39] Zhiliang Peng, Li Dong, Hangbo Bao, Qixiang Ye, and Furu Wei. A unified view of masked image modeling. *arXiv preprint arXiv:2210.10615*, 2022. 6
- [40] Mary Phuong and Christoph H Lampert. Distillation-based training for multi-exit architectures. In *Proceedings of the IEEE/CVF International Conference on Computer Vision*, pages 1355–1364, 2019. 1, 2
- [41] Alec Radford, Jong Wook Kim, Chris Hallacy, Aditya Ramesh, Gabriel Goh, Sandhini Agarwal, Girish Sastry, Amanda Askell, Pamela Mishkin, Jack Clark, et al. Learning transferable visual models from natural language supervision. In *International Conference on Machine Learning*, pages 8748–8763. PMLR, 2021. 5, 6, 8, 16
- [42] Piyush Sharma, Nan Ding, Sebastian Goodman, and Radu Soricut. Conceptual captions: A cleaned, hypernymed, image alt-text dataset for automatic image captioning. In *Proceedings of the 56th Annual Meeting of the Association for Computational Linguistics (Volume 1: Long Papers)*, pages 2556–2565, 2018. 16
- [43] Seungwoo Son, Namhoon Lee, and Jaeho Lee. Maskedkd: Efficient distillation of vision transformers with masked images. *arXiv preprint arXiv:2302.10494*, 2023. 2
- [44] Nitish Srivastava, Geoffrey Hinton, Alex Krizhevsky, Ilya Sutskever, and Ruslan Salakhutdinov. Dropout: a simple way to prevent neural networks from overfitting. *The Journal of Machine Learning Research*, 15(1):1929–1958, 2014. 2, 4, 8, 14, 15
- [45] Hugo Touvron, Matthieu Cord, Matthijs Douze, Francisco Massa, Alexandre Sablayrolles, and Hervé Jégou. Training data-efficient image transformers & distillation through attention. In *International Conference on Machine Learning*, pages 10347–10357. PMLR, 2021. 1, 2, 4, 5
- [46] Hugo Touvron, Matthieu Cord, Alexandre Sablayrolles, Gabriel Synnaeve, and Hervé Jégou. Going deeper with image transformers. In *Proceedings of the IEEE/CVF International Conference on Computer Vision*, pages 32–42, 2021. 16
- [47] Hugo Touvron, Matthieu Cord, and Hervé Jégou. Deit iii: Revenge of the vit. In *Proceedings of the European Conference on Computer Vision*, pages 516–533. Springer, 2022. 1, 2, 3, 4, 5, 7, 15, 16, 17
- [48] Hugo Touvron, Matthieu Cord, Maxime Oquab, Piotr Bojanowski, Jakob Verbeek, and Hervé Jégou. Co-training 2^L submodels for visual recognition. *arXiv preprint arXiv:2212.04884*, 2022. 2, 5, 7
- [49] Grant Van Horn, Oisín Mac Aodha, Yang Song, Yin Cui, Chen Sun, Alex Shepard, Hartwig Adam, Pietro Perona, and Serge Belongie. The inaturalist species classification and detection dataset. In *Proceedings of the IEEE conference on computer vision and pattern recognition*, pages 8769–8778, 2018. 7, 8, 16
- [50] Alex Wang, Amanpreet Singh, Julian Michael, Felix Hill, Omer Levy, and Samuel R Bowman. Glue: A multi-task benchmark and analysis platform for natural language understanding. *arXiv preprint arXiv:1804.07461*, 2018. 8, 16
- [51] Xiao Wang, Haoqi Fan, Yuandong Tian, Daisuke Kihara, and Xinlei Chen. On the importance of asymmetry for siamese representation learning. In *Proceedings of the IEEE/CVF Conference on Computer Vision and Pattern Recognition*, pages 16570–16579, 2022. 2

- [52] Longhui Wei, Lingxi Xie, Wengang Zhou, Houqiang Li, and Qi Tian. Mvp: Multimodality-guided visual pre-training. In *European Conference on Computer Vision*, pages 337–353. Springer, 2022. 6
- [53] Yixuan Wei, Han Hu, Zhenda Xie, Zheng Zhang, Yue Cao, Jianmin Bao, Dong Chen, and Baining Guo. Contrastive learning rivals masked image modeling in fine-tuning via feature distillation. *arXiv preprint arXiv:2205.14141*, 2022. 6
- [54] Ross Wightman, Hugo Touvron, and Hervé Jégou. Resnet strikes back: An improved training procedure in timm. *arXiv preprint arXiv:2110.00476*, 2021. 1, 2, 3, 5, 6, 7
- [55] Sanghyun Woo, Shoubhik Debnath, Ronghang Hu, Xinlei Chen, Zhuang Liu, In So Kweon, and Saining Xie. Convnext v2: Co-designing and scaling convnets with masked autoencoders. *arXiv preprint arXiv:2301.00808*, 2023. 6
- [56] Yuxin Wu, Alexander Kirillov, Francisco Massa, Wan-Yen Lo, and Ross Girshick. Detectron2. <https://github.com/facebookresearch/detectron2>, 2019. 16
- [57] Tete Xiao, Yingcheng Liu, Bolei Zhou, Yuning Jiang, and Jian Sun. Unified perceptual parsing for scene understanding. In *Proceedings of the European Conference on Computer Vision (ECCV)*, pages 418–434, 2018. 13
- [58] Saining Xie, Ross Girshick, Piotr Dollár, Zhuowen Tu, and Kaiming He. Aggregated residual transformations for deep neural networks. In *Proceedings of the IEEE conference on computer vision and pattern recognition*, pages 1492–1500, 2017. 6
- [59] Chuanguang Yang, Zhulin An, Helong Zhou, Linhang Cai, Xiang Zhi, Jiwen Wu, Yongjun Xu, and Qian Zhang. Mixskd: Self-knowledge distillation from mixup for image recognition. In *European Conference on Computer Vision*, pages 534–551. Springer, 2022. 6
- [60] Taojiannan Yang, Sijie Zhu, and Chen Chen. Gradaug: A new regularization method for deep neural networks. *Advances in Neural Information Processing Systems*, 33: 14207–14218, 2020. 7
- [61] Jiahui Yu, Linjie Yang, Ning Xu, Jianchao Yang, and Thomas Huang. Slimmable neural networks. *arXiv preprint arXiv:1812.08928*, 2018. 7
- [62] Linfeng Zhang, Jiebo Song, Anni Gao, Jingwei Chen, Chenglong Bao, and Kaisheng Ma. Be your own teacher: Improve the performance of convolutional neural networks via self distillation. In *Proceedings of the IEEE/CVF International Conference on Computer Vision*, pages 3713–3722, 2019. 1, 2, 6
- [63] Linfeng Zhang, Chenglong Bao, and Kaisheng Ma. Self-distillation: Towards efficient and compact neural networks. *IEEE Transactions on Pattern Analysis and Machine Intelligence*, 44(8):4388–4403, 2021. 6
- [64] Xinyu Zhang, Jiahui Chen, Junkun Yuan, Qiang Chen, Jian Wang, Xiaodi Wang, Shumin Han, Xiaokang Chen, Jimin Pi, Kun Yao, et al. Cae v2: Context autoencoder with clip latent alignment. *Transactions on Machine Learning Research*, 2023. 6
- [65] Ying Zhang, Tao Xiang, Timothy M Hospedales, and Huchuan Lu. Deep mutual learning. In *Proceedings of the IEEE conference on computer vision and pattern recognition*, pages 4320–4328, 2018. 2, 7
- [66] Zhun Zhong, Liang Zheng, Guoliang Kang, Shaozi Li, and Yi Yang. Random erasing data augmentation. In *Proceedings of the AAAI conference on artificial intelligence*, pages 13001–13008, 2020. 1, 16
- [67] Bolei Zhou, Hang Zhao, Xavier Puig, Sanja Fidler, Adela Barriuso, and Antonio Torralba. Scene parsing through ade20k dataset. In *Proceedings of the IEEE/CVF Conference on Computer Vision and Pattern Recognition*, pages 633–641, 2017. 13
- [68] Xiatian Zhu, Shaogang Gong, et al. Knowledge distillation by on-the-fly native ensemble. *Advances in neural information processing systems*, 31, 2018. 1, 2, 6

Appendix

A. Experiments

A.1. Training budget

We report an extensive comparison of the training budget in addition to Table 7. Table A.1 shows the performance improvements of MaskSub compared to training recipes with increased epochs to have the same training costs as MaskSub. In most cases, MaskSub outperforms its counterparts even with the same training computation costs. The results imply that MaskSub is a better solution than increasing training epochs to improve model performance. Note that the performance of MAE finetuning is lower than the original epoch since it utilizes benefits from early stop training to prevent overfitting.

	Architecture	Training recipe	+MaskSub	Epochs	GPU days	Accuracy
DeiT-III Training	ViT-S/16	DeiT-III	-	600	22	80.7
			✓	400	22	81.2 (+0.5)
	DeiT-III	DeiT-III	-	1200	45	81.6
			✓	800	44	81.7 (+0.1)
	ViT-B/16	DeiT-III	-	600	26	83.7
			✓	400	25	84.1 (+0.4)
DeiT-III	DeiT-III	-	1200	52	83.8	
		✓	800	50	84.2 (+0.4)	
MAE Finetuning	ViT-B/16	MAE Finetune	-	150	9	83.5
			✓	100	9	83.9 (+0.4)
MAE Finetuning	ViT-L/16	MAE Finetune	-	75	14	85.5
			✓	50	14	86.1 (+0.6)
ResNet Training	ResNet50	RSB A1	-	600	22	80.4
			✓	300	14	80.0 (-0.4)
	ResNet101	RSB A1	-	600	24	81.5
			✓	300	20	82.1 (+0.6)
	ResNet152	RSB A1	-	600	32	82.0
			✓	300	29	82.8 (+0.8)

Table A.1. **Comparison in the same training budget.** All training has been conducted with NVIDIA V100 8 GPUs. GPU days refer to the number of days required for training when using a single V100 GPU.

A.2. Downstream tasks

Semantic segmentation. Following the training setup of the ADE-20k semantic segmentation (provided in BEiT v2 [38]), we train UpperNet [57] with the ViT backbones on ADE-20k [67]. Table A.2 shows the results of single-scale and multi-scale evaluations. On both evaluations, the backbone pretrained with MaskSub demonstrates superior performance, consistent for the ViT-B and ViT-L backbones.

Object detection and instance segmentation. We utilize Cascaded Mask R-CNN [3] with the ViT backbones [33] for MS COCO [35], which conducts object detection and instance segmentation simultaneously. ViTDet [33] is used as a training recipe for this experiment. Table A.3 shows the results. The metric AP^{box} quantifies the performance in object detection, while AP^{mask} provides performance in instance segmentation. In both measures, the backbone pretrained with MaskSub outperforms the DeiT-III backbone.

	Single-scale mIoU		Multi-scale mIoU	
	DeiT-III	+ MaskSub	DeiT-III	+ MaskSub
ViT-B	48.8	49.4 (+0.6)	49.7	50.2 (+0.5)
ViT-L	51.7	52.2 (+0.5)	52.3	52.7 (+0.4)

Table A.2. **Semantic segmentation on ADE-20k.** UpperNet for ViT backbone is trained with the BEiT v2 segmentation recipe.

	AP^{box}	AP^{mask}
DeiT-III	50.7	43.6
+MaskSub	50.9 (+0.2)	43.9 (+0.3)

Table A.3. **Detection and instance segmentation on MS COCO.** Cascaded Mask R-CNN with ViT-B is used.

A.3. Robustness

We evaluate the impact of MaskSub in various robustness benchmarks. We use models trained for 800 epochs in Table 1. Table A.4 shows the results. ViT models trained with MaskSub demonstrate superior performance in in-distribution metrics and all out-of-distribution metrics. Specifically, MaskSub outperforms each baseline in natural adversarial examples (IN-A [24]), objects in different styles and textures (IN-R [23]), controls in rotation, background, and viewpoints (ObjNet [2]), and detecting spurious correlations with background [13] (SI-size, SI-loc, and SI-rot). The results demonstrate that the improvement of MaskSub is not limited to the ImageNet-1k validation and has been verified across various robustness metrics.

Model	+MaskSub	IN-1k	IN-V2	IN-Real	IN-A	IN-R	ObjNet	SI-size	SI-loc	SI-rot
ViT-S	-	81.4	70.1	87.0	23.4	46.4	32.6	55.0	39.8	37.8
	✓	81.7	71.0	87.4	26.9	47.2	33.5	56.7	42.5	39.9
ViT-B	-	83.8	73.4	88.2	36.8	54.1	35.7	58.0	42.7	41.5
	✓	84.2	74.0	88.6	41.9	54.4	37.2	59.0	44.8	43.3
ViT-L	-	84.9	74.8	88.8	45.3	57.4	38.8	59.8	46.5	45.0
	✓	85.3	75.8	89.2	51.1	58.5	40.0	60.2	46.8	45.9
ViT-H	-	85.2	75.7	89.2	51.9	58.8	40.1	61.9	49.0	46.8
	✓	85.7	76.5	89.6	58.3	59.9	41.7	62.4	50.1	48.4

Table A.4. **Robustness benchmark.** Table shows the robustness benchmark for ViT pretrained with/without MaskSub. In all metrics, higher scores indicate better results.

A.4. Extending to drop regularizations

To generalize MaskSub to drop regularizations, we demonstrate MaskSub with drop-out [44] (DropSub) and drop-path [27] (PathSub) in Table 13. In this section, we present additional analysis to verify MaskSub variants. The experiment setup is the same as in Section 3.2. The results are shown in Table A.5. We validate three MaskSub methods for three kinds of regularizations: random masking [21], drop-out [44], and drop-path [27]. “Original” means the original training recipe trained with Eq. 1, and none of the drop regularizations is used. “Single model” shows the performance when the network is trained with Eq. 2. Note that it is a common practice to use drop-based techniques. We compare those common practices with “MaskSub variants”, models trained with Eq. 1 and 3. For analysis, we measured Eq. 1 “train loss (original)” and Eq. 2 “train loss (drop)” regardless of the loss used for training. It shows how losses changed by training setting. The results demonstrate that MaskSub improves training in all three cases. In all cases, MaskSub improves original and drop loss convergence, which is connected to superior accuracy compared to original training.

	Drop ratio	Single model			MaskSub variants		
		Accuracy	Train loss (original)	Train loss (drop)	Accuracy	Train loss (original)	Train loss (drop)
Original	-	77.4	6.42	-	-	-	-
Masking [21]	25%	76.3	6.60	6.96	79.0	5.89	6.38
	50%	73.8	7.02	7.77	79.4	5.81	6.89
	75%	67.3	8.08	9.27	79.2	5.84	8.15
Drop-out [44]	0.1	76.1	6.60	6.87	79.1	5.88	6.32
	0.2	74.1	6.95	7.34	79.1	5.82	6.57
	0.3	71.6	8.34	7.79	79.1	5.84	6.90
Drop-path [27]	0.1	77.4	6.42	6.42	78.4	6.11	6.11
	0.2	74.9	6.74	7.19	78.7	5.91	6.48
	0.3	71.6	7.31	8.04	78.8	5.87	7.02

Table A.5. **Analysis with drop regularizations.** This table shows 100 epochs of the ViT-B performance trained with drop regularizations. Note that training loss scale 10^{-3} is omitted for simplicity. The table presents the average values over three separate runs, and the standard deviations are reported in Table A.11. We observe that MaskSub consistently enhances the baselines significantly and also decreases the training loss at the main branch. This suggests that our method effectively facilitates training with regularizations.

A.5. Ablation studies

We conduct ablation studies of MaskSub using DeiT-III training settings to validate the role of KD loss and the effects of hyperparameters. Table A.6 shows the impacts of KD loss in MaskSub. Performance improvement by MaskSub is significantly limited when KD loss is not used. Analysis for masking ratio and loss weights are shown in Table A.7 and Table A.8 respectively. Note that we use DeiT-III 100 epochs setting and baseline without MaskSub is 77.4.

	Baseline	MaskSub	
		w/o KD loss	with KD loss
ViT-S/16	80.4	80.5 (+0.1)	81.1 (+0.7)
ViT-B/16	83.5	83.6 (+0.1)	84.1 (+0.6)

Table A.6. **Effect of KD loss.** We analyze removing KD loss of the sub-model. We use the DeiT-III 400 epochs setting as in Table 1.

Mask ratio	0%	25%	40%	50%	60%	75%						
Accuracy	78.4	79.0	79.2	79.2	79.3	79.2						
Costs	$\times 2.0$	$\times 1.75$	$\times 1.6$	$\times 1.5$	$\times 1.4$	$\times 1.25$						
							Weights (CE, KD) (1, 0) $(\frac{3}{4}, \frac{1}{4})$ $(\frac{2}{3}, \frac{1}{3})$ $(\frac{1}{2}, \frac{1}{2})$ $(\frac{1}{3}, \frac{2}{3})$ $(\frac{1}{4}, \frac{3}{4})$					
							Accuracy 77.4 78.5 78.7 79.2 79.2 78.5					

Table A.7. **Mask ratio.** Table shows MaskSub with various mask ratios using DeiT-III ViT-B/16 100 epochs setting.

Table A.8. **Loss weights.** Different loss weights are compared using ViT-B/16 with 100 epochs setting. Note that MaskSub uses $(\frac{1}{2}, \frac{1}{2})$.

A.6. Reporting mean and standard deviation

We provide mean and standard deviation for experiments using different random seeds. The values presented in this section result from three independent runs with different seeds.

Mean and standard deviation values for transfer learning in Table 10 are shown in Table A.9. MaskSub demonstrates significant gains, which surpass the standard deviation of performance. Table A.10 presents short training (300 epochs) results. MaskSub shows substantial improvements when it is applied to both pretraining and finetuning processes.

Table A.12 shows 400 epochs training with DeiT-III [47], which is reported in Table 13 of the paper. MaskSub variants improve the performance of ViT training. Compared to the variants, MaskSub demonstrates the best performance.

Table A.11 shows the mean and standard deviation values for Table A.5. Table A.11 shows the superiority of our MaskSub in additional regularization training.

Model	Pretraining + MaskSub	Finetuning + MaskSub	CIFAR10	CIFAR100	Flowers	Cars	iNat-18	iNat-19
ViT-S	-	-	98.83 ± 0.05	89.96 ± 0.15	94.54 ± 1.71	80.86 ± 0.71	70.12 ± 0.13	76.69 ± 0.56
	✓	-	98.88 ± 0.09	90.63 ± 0.09	95.19 ± 1.95	81.23 ± 0.73	70.82 ± 0.03	77.00 ± 0.21
	✓	✓	98.77 ± 0.05	89.87 ± 0.17	98.25 ± 0.51	92.17 ± 0.14	71.17 ± 0.21	77.12 ± 0.48
ViT-B	-	-	99.07 ± 0.05	91.69 ± 0.15	97.52 ± 0.51	90.05 ± 0.24	73.16 ± 0.05	78.49 ± 0.62
	✓	-	99.19 ± 0.03	91.89 ± 0.04	97.73 ± 0.30	90.18 ± 0.12	73.61 ± 0.08	78.77 ± 0.05
	✓	✓	98.82 ± 0.03	89.55 ± 0.05	98.68 ± 0.16	92.77 ± 0.09	73.88 ± 0.12	79.07 ± 0.55

Table A.9. Mean and std for transfer learning to small scale datasets. Table shows ‘mean ± std’ values for transfer learning performance with/without MaskSub. We measure the performance when MaskSub is applied to pretraining and finetuning.

Model	Pretraining + MaskSub	Finetuning + MaskSub	CIFAR10	CIFAR100	Flowers	Cars
ViT-S	-	-	98.41 ± 0.12	87.27 ± 0.19	66.66 ± 2.52	46.04 ± 3.72
	✓	-	98.48 ± 0.06	87.54 ± 0.33	72.61 ± 1.20	45.46 ± 1.80
	✓	✓	98.96 ± 0.06	90.81 ± 0.09	96.64 ± 0.23	87.43 ± 0.43
ViT-B	-	-	98.97 ± 0.10	90.33 ± 0.14	90.92 ± 1.60	78.52 ± 0.59
	✓	-	99.06 ± 0.02	90.82 ± 0.21	92.45 ± 0.90	80.34 ± 0.56
	✓	✓	99.15 ± 0.04	91.52 ± 0.16	98.44 ± 0.13	92.22 ± 0.03

Table A.10. Transfer learning at short (300 epochs) training. Table shows ‘mean ± std’ values for transfer learning at 300 epochs. We measure the performance when MaskSub is applied to pretraining and finetuning.

	Drop ratio	Single model			Sub-model training (MaskSub)		
		Accuracy	Train loss (original)	Train loss (drop)	Accuracy	Train loss (original)	Train loss (drop)
Original	-	77.40 ± 0.20	6.42 ± 0.03	-	-	-	-
Masking [21]	25%	76.33 ± 0.28	6.60 ± 0.05	6.96 ± 0.05	79.02 ± 0.12	5.89 ± 0.03	6.38 ± 0.04
	50%	73.78 ± 0.08	7.02 ± 0.04	7.77 ± 0.03	79.36 ± 0.01	5.81 ± 0.01	6.89 ± 0.01
	75%	67.27 ± 0.25	8.08 ± 0.05	9.27 ± 0.04	79.16 ± 0.05	5.84 ± 0.01	8.15 ± 0.02
Drop-out [44]	0.1	76.09 ± 0.25	6.60 ± 0.07	6.87 ± 0.06	79.14 ± 0.15	5.88 ± 0.02	6.32 ± 0.02
	0.2	74.10 ± 0.22	6.95 ± 0.06	7.34 ± 0.06	79.10 ± 0.11	5.82 ± 0.04	6.57 ± 0.04
	0.3	71.62 ± 0.29	8.34 ± 0.03	7.79 ± 0.03	79.09 ± 0.15	5.84 ± 0.03	6.90 ± 0.03
Drop-path [27]	0.1	77.40 ± 0.20	6.42 ± 0.03	6.42 ± 0.03	78.36 ± 0.03	6.11 ± 0.01	6.11 ± 0.01
	0.2	74.92 ± 0.12	6.74 ± 0.04	7.19 ± 0.03	78.72 ± 0.12	5.91 ± 0.01	6.48 ± 0.01
	0.3	71.57 ± 0.10	7.31 ± 0.02	8.04 ± 0.02	78.80 ± 0.15	5.87 ± 0.02	7.02 ± 0.01

Table A.11. Mean and std for analysis on drop regularization with/without MaskSub. The table shows ‘mean ± std’ values for experiments in Table A.5 of the paper. Note that training loss scale 10^{-3} is omitted for simplicity.

Architecture	Baseline	DropSub	PathSub	MaskSub
ViT-S/16	80.40 \pm 0.33	80.57 \pm 0.12	80.78 \pm 0.05	81.08 \pm 0.12
ViT-B/16	83.46 \pm 0.04	83.83 \pm 0.11	83.80 \pm 0.12	84.08 \pm 0.02

Table A.12. **Mean and std for three variants of MaskSub.** We report ‘mean \pm std’ values for 400 epochs training with DeiT-III [47]. Note that we use the performance of the original paper [47] for baseline training.

B. Implementation details

Most experiments in the paper were performed on a machine with NVIDIA V100 8 GPUs. The exceptions were DeiT-III [47] experiments for ViT-L and ViT-H in Table 1 and object detection in Table A.3, conducted with NVIDIA A100 64 GPUs. Also, we use a single NVIDIA V100 for transfer learning in Table 10. We strictly follow original training recipes for experiments. We denote details of the training recipes to clarify our implementation details and assist in reproducing our results.

Image Classification. Table B.1 shows training recipes used for Table 1, 3, 5, 8, 9, and 13 of the paper. It demonstrates that our MaskSub is validated on various training recipes that cover diverse regularization and optimizer settings and achieves consistent improvement on all settings, which exhibits the general applicability of MaskSub. Note that MaskSub is applied to all recipes with the same masking ratio of 50%. Thus, MaskSub does not require hyper-parameter tuning specialized for each recipe. Model-specific training recipes of DeiT-III [47] are reported in Table B.2. DeiT-III achieves strong performance with sophisticatedly tuned training parameters mainly focused on input size and drop-path rate. It makes improving DeiT-III more challenging than other recipes, yet our MaskSub accomplishes this with a significant performance gap.

Semantic segmentation. We use the BEiT v2’s segmentation recipe [38] that utilizes MMCV [8] and MMSeg [9] library. Following the default setting, we replace the ViT backbone with the DeiT-III backbone, which includes layer-scale [46]. Then, we train the segmentation task for 160k iteration using DeiT-III and DeiT-III + MaskSub pretrained backbone.

Object detection and instance segmentation We use Detectron2 [56] on the COCO [35] dataset. Among various recipes in the Detectron2 library, we use ViTDet [33], which is a recent and strong recipe for a ViT-based detector. We train ViTDet Cascaded Mask-RCNN with DeiT-III and DeiT-III + MaskSub pretrained backbone and report performance after MSCOCO 100 epoch training.

Transfer learning. We use the AdamW training recipe on DeiT-III [47] transfer learning. We use lr 10^{-5} , weight-decay 0.05, batch size 768. Drop-path [27] and random erasing [66] are not used. Data augmentation is set to be the same as DeiT-III, and we train ViT for 1000 epochs with a cosine learning rate decay. For CIFAR datasets, we resize 32×32 image to 224×224 to use the ImageNet pretrained backbones. In the case of the iNaturalist datasets [49], we use AdamW with lr 7.5×10^{-5} , weight-decay 0.05, batch size 768. Drop-path and random erasing ratios are set to 0.1, and ViT is trained for 360 epochs with cosine learning rate decay.

Text classification. We use the HuggingFace open-source code for the GLUE benchmark [50]. Random masking is implemented using the masking part of the HuggingFace BERT [12], which replaces random tokens with a mask token. Following the BERT pretraining, we set a random masking ratio to 15%, and only replacing tokens to the mask token is applied to randomly selected tokens.

CLIP pretraining. In pretraining, CLIP [41] encodes N image-text pairs of a batch and builds an $N \times N$ similarity matrix. Using contrastive learning loss, CLIP is trained to have high similarity for matched image-text pairs and low similarity for unmatched pairs. Implementing MaskSub upon CLIP is straightforward since the contrastive learning loss also utilizes *cross-entropy loss* over the similarity matrix. In the experiment, we only mask images, not texts. The difference between the “main-model” and “sub-model” is that the “sub-model” receives 50% masked images, and the “sub-model” is trained to mimic the similarity matrix of the “main-model” for the same batch. We use OPEN-CLIP¹ codebase for the CLIP pretraining. We follow the codebase’s default training recipes. We train CLIP ViT-B/32 with a batch size of 1,024 using 8 NVIDIA V100 GPUs. Training datasets are CC3M [42], CC12M [5], and RedCaps [11]. The number of seen samples during training is 128M.

¹https://github.com/mlfoundations/open_clip

Training recipe	DeiT-III	RSB A2	Swin	MAE	BEiT v2	FT-CLIP
Fine-tuning	X	X	X	✓	✓	✓
Epoch	400 / 800	300	300	100, 50	100, 50	50, 30
Batch size	2048	2048	1024	1024	1024	2048
Optimizer	LAMB	LAMB	AdamW	AdamW	AdamW	AdamW
LR	3×10^{-3}	5×10^{-3}	1×10^{-3}	$(2, 4) \times 10^{-3}$	$(5, 2) \times 10^{-4}$	$(6, 4) \times 10^{-4}$
LR decay	cosine	cosine	cosine	cosine	cosine	cosine
Layer LR decay	-	-	-	0.65, 0.75	0.6, 0.8	0.6, 0.65
Weight decay	0.03 / 0.05	0.01	0.05	0.05	0.05	0.05
Warmup epochs	5	5	20	5	20, 5	10, 5
Loss	BCE	BCE	CE	CE	CE	CE
Label smoothing	-	-	0.1	0.1	0.1	0.1
Dropout	-	-	-	-	-	-
Drop-path	Table B.2	0.05	0.1	0.1, 0.2, 0.3	0.2	-
Repeated aug	✓	✓	-	-	-	-
Gradient clip	1.0	-	5.0	-	-	-
RandAugment	Three Aug.	7 / 0.5	9 / 0.5	9 / 0.5	9 / 0.5	9 / 0.5
Mixup alpha	0.8	0.1	0.8	0.8	0.8	-
CutMix alpha	1.0	1.0	1.0	1.0	1.0	-
Random erasing	-	-	0.25	0.25	0.25	0.25
Color jitter	0.3	-	0.4	-	0.4	0.4
EMA	-	-	-	-	-	0.9998
Train image size	Table B.2	224×224	224×224	224×224	224×224	224×224
Test image size	224×224	224×224	224×224	224×224	224×224	224×224
Test crop ratio	1.0	0.95	0.875	0.875	0.875	1.0

Table B.1. **Details of various training recipes used for experiments.** Our MaskSub achieves consistent improvement in all training recipes, which covers diverse regularization and optimizer settings.

		400 epochs				800 epochs			
		ViT-S	ViT-B	ViT-L	ViT-H	ViT-S	ViT-B	ViT-L	ViT-H
Pretraining	Image size	224	192	192	160	224	192	192	160
	Drop-path	0.0	0.1	0.4	0.5	0.05	0.2	0.45	0.6
	LR	0.004		0.003		0.004		0.003	
	Weight decay			0.03				0.05	
	Drop-path	-	0.2	0.45	0.55	-	0.2	0.45	0.55
Resolution	Epochs	-		20		-		20	
Finetuning	Image size	-		224×224		-		224×224	
	Optimizer	-		AdamW		-		AdamW	
	LR	-		$1e-5$		-		$1e-5$	

Table B.2. **Model specific recipes of DeiT-III [47].** The table shows model size and training length-specific training arguments used for the DeiT-III recipe. In addition to Table B.1, DeiT-III utilizes drop-path and image size to adjust the recipe for diverse model sizes and training lengths.